Magnetoresistance and Domain Structure in Thin Nickel Films*

RICHARD L. COREN† AND HELLMUT J. JURETSCHKE
Polytechnic Institute of Brooklyn, Brooklyn, New York
(Received December 28, 1961)

Magnetoresistance measurements have been used to determine the magnetic domain structure of nickel films. The magnetoresistance results are discussed in terms of a new representation in which the resistivity components parallel and transverse to the current, measured simultaneously as the applied magnetic field varies in magnitude or direction, are regarded as Cartesian coordinates. This representation is independent of the direction of the current relative to any preferred orientations in the film. Marked differences are found between the measured magnetoresistance and the behavior expected of a single-domain film. The nature of the differences indicates that these films must at least contain an angular distribution of uniaxial magnetic regions in the film plane. A particular model having these properties is developed. Here local anisotropy axes are uniformly distributed in direction and are superimposed on a common uniaxial anisotropy. The local and common anisotropy energies are assumed of different strength; their ratio K is regarded as a parameter. The magnetic behavior of the model is easily studied for a complete range of K values, because the model can be transformed into an equivalent distribution of singly uniaxial domains with a nonuniform distribution of axial directions about the common axis of the film and a corresponding range of equivalent anisotropy strengths. The magnetoresistance for this model is computed numerically and found to be in over-all agreement with the measurements. It is shown that a distribution of K values can account for the remaining quantitative differences between experiment and the model.

I. INTRODUCTION

THE anomalies in the electrical behavior of ferromagnetic metals related to the magnetization of the material provide a method for studying magnetic properties by means of electrical measurements. Though the relation between the two sets of phenomena is not fully understood, the dependence of the electrical properties of a single domain on the magnetization direction relative to that of the current follows from symmetry requirements imposed by the structure of the material and the nature of the vectors entering Ohm's law. The simplest phenomenological form of Ohm's law, for an isotropic or polycrystalline material with a uniform magnetization $\mathbf{M}$, is given by[1]

$$\mathbf{E}=\rho_\perp\mathbf{J}+[(\rho_{11}-\rho_\perp)/M_0^2](\mathbf{J}\cdot\mathbf{M})\mathbf{M}-(\rho_H/M_0)\mathbf{J}\times\mathbf{M}. \quad (1)$$

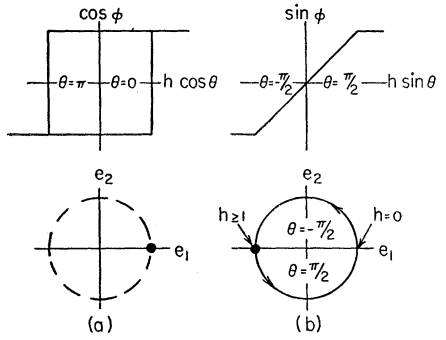

FIG. 1. Conventional hysteresis loops of a single uniaxial domain, and their magnetoresistance representation. (a) field along preferred axis $\theta=0$, π; (b) field in the hard direction, $\theta=\pm\pi/2$.

* Supported by the Office of Naval Research. Part of a thesis submitted by Richard L. Coren in partial fulfillment of the requirements for the degree of Doctor of Philosophy at the Polytechnic Institute of Brooklyn.

† Now at: Philco Scientific Laboratory, Blue Bell, Pennsylvania.

[1] J. P. Jan, *Solid-State Physics*, edited by F. Seitz and D. Turnbull (Academic Press Inc., New York, 1957), Vol. 5.

ρ_{11} and $\rho_\perp$ are the longitudinal resistivities for $\mathbf{M}$ parallel and normal to $\mathbf{J}$, ρ_H is the extraordinary Hall resistivity, $M_0=|\mathbf{M}|$. Equation (1) omits the corresponding effects proportional to $\mathbf{B}$ which become important only at very high fields.

The material parameters ρ_{11}, $\rho_\perp$, ρ_H usually are functions of temperature and perhaps of other variables not involving $\mathbf{M}$. Thus, for known parameters in Eq. (1), the direction of $\mathbf{M}$ is specified by electrical measurements. In multidomain samples such measurement gives averages of the magnitude and direction of $\mathbf{M}$ often simply weighted by the total fractions of each orientation present and thus related to the technical magnetization. Among the advantages of the use of electrical measurements to study magnetic properties are the following: They refer to the instantaneous magnetic state and in no way interfere with this state; in some experimental situations they may be done more simply than direct magnetic measurements, and in multidomain samples they complement such direct measurements because they see a different average. On the other hand, they always depend on interpretation in terms of a phenomenological relation such as Eq. (1) and on an averaging process applied to a multidomain model which may be neither exact nor unique.

The usefulness of the method has been verified in bulk samples by Foner[2] who used the extraordinary Hall effect to study the approach to saturation in iron, and by Bozorth[3] who explained the resistance variation of stressed ferromagnetic specimens in terms of changes of their domain structure. Recently interest has been shown in extending this approach to ferromagnetic films.[4–6] We apply it here to the study of magnetization

[2] S. Foner, Phys. Rev. **95**, 652 (1954).
[3] R. Bozorth, Phys. Rev. **70**, 923 (1946).
[4] L. Reimer, Z. Naturforsch. **12A**, 550 (1957).
[5] Z. F. Hellenthal, Z. Physik **153**, 359 (1958).
[6] T. Rappeneau, Cahiers phys. **12**, 185 (1958).

changes occurring in very thin films of nickel with variations of an external field in the film plane. Except at very high fields, the measurements require interpretation in terms of a multidomain structure. However, their salient features imply a domain structure with certain well-defined characteristics, and we present a simple model whose predicted electrical properties compare well with the experimental results.

II. MAGNETORESISTANCE REPRESENTATION OF SINGLE-DOMAIN MAGNETIC BEHAVIOR

The behavior of a single domain forms a convenient, experimentally realizable, reference state for analyzing more complex observations. This section deals with the electrical representation of typical cyclical paths of the magnetization of a single domain.

For a film in the x–y plane, with **J** along x, and **M** in the film plane making an angle ϕ_1 with **J**, the two measurable components of Eq. (1) are

$$\begin{aligned} e_1 &= E_x/J_x = \rho + \Delta\rho \cos 2\phi_1, \\ e_2 &= E_y/J_x = \Delta\rho \sin 2\phi_1, \end{aligned} \tag{2}$$

where

$$\rho = \tfrac{1}{2}(\rho_{11}+\rho_1), \quad \Delta\rho = \tfrac{1}{2}(\rho_{11}-\rho_1). \tag{3}$$

In the e_1–e_2 plane, Eq. (2) defines the locus of the magnetoresistance point $\mathbf{P}=(e_1,e_2)$ as a circle of radius $\Delta\rho$, centered at $(\rho,0)$. **M** lies along the axis bisecting the radial angle of **P** and the x axis and, except for the ambiguity in polarity, the direction and motion of **M** in the film plane are directly related to the location and path traced by **P** along the circle.

Consider the rotational behavior of **M** in a uniaxial single domain. With a field intensity **H** in the film plane, **M** is directed so as to minimize the magnetic free energy,

$$F = K \sin^2\phi_2 - HM \cos(\theta-\phi_2), \tag{4}$$

where θ and ϕ_2 are the angles of **H** and **M** with respect to the preferred anisotropy direction, and K is the uniaxial anisotropy energy. Equilibrium is defined by

$$\sin 2\phi_2 = 2h \sin(\theta-\phi_2), \tag{5}$$

conveniently written in terms of the reduced field

$$h = H/H_K = HM/2K. \tag{6}$$

Equation (5) determines $\phi_2(h,\theta)$. $\phi_1(h,\theta)$ follows once the direction ξ of the uniaxial easy axis with respect to the current is known: $\phi_1=\xi+\phi_2$. Since the only effect of ξ is to rotate the circle of **P** about its center, leaving the trace unchanged otherwise, no generality is lost by setting $\xi=0$, and dropping the subscripts on the angles ϕ. If $\phi_1 \neq \phi_2$, the figures derived below must be rotated through 2ξ and θ is then measured with respect to a different origin.

The variation of ϕ with h and θ is well known.[7] If h is brought along the preferred direction ($\theta=0$) from a large value to zero and then increased in the opposite sense, **M** remains at $\phi=0$ for small reverse h and switches to $\phi=\pi$ when $h=1$, $\theta=\pi$, producing the square hysteresis loop of Fig. 1(a). If **H** is along $\theta=\pi/2$, **M** rotates from $\phi=\pi/2$ for $h\geq 1$ to $\phi=0$ at $h=0$, and continues to $\phi=-\pi/2$ as h increases to unity at $\theta=-\pi/2$, giving the closed reversible loop in the hard direction, shown in Fig. 1(b).

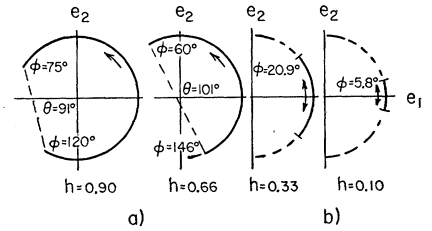

FIG. 2. Magnetoresistance traces of a single uniaxial domain for rotating fields of constant magnitude. The field angles θ, and the angles ϕ, indicate points of switching ($h=0.90$, 0.66), or maximum excursion ($h=0.33$, 0.10). For $h>1$ the full circle is traced.

The corresponding traces of **P** follow from Eq. (2) and are also shown in Fig. 1. For convenience the origin of the e_1–e_2 plane has been shifted to $(\rho,0)$ and the radius of the circle is normalized. The mapping $\phi \rightarrow 2\phi$ predicts that during the entire cycle giving the square hysteresis loop of (a) **P** remains stationary at $(e_1,e_2)=(1,0)$, while, for $\theta=\pm\pi/2$, **P** traces the full circle in the range $h\leq 1$, as shown in (b).

More revealing cycles of **M** and **P** are obtained by varying θ through all angles at constant h. Here the traces fall into three groups. With high fields ($h>1$), **H** and **M** are always nearly parallel, so that **P** traces out the entire circle twice for a full turn of **H**. At smaller h we will specify the initial condition as $\phi=0$ at $\theta=0$. When $1>h>\frac{1}{2}$, **M** lags behind **H** and ϕ reaches a switching angle at less than $\pi/2$. Upon further increase of θ, **M** switches to a new equilibrium position on the other side of the uniaxial hard direction, causing **P** to jump along the circle; as **M** rotates further, **P** completes the circular segment, always moving in the same direction. For a full rotation of h, the segment is traversed twice. Such paths of **P** for $h=0.90$, and 0.66 are shown in Fig. 2(a); the dashed lines connect initial and final locations of **P** at switching. For $h<\frac{1}{2}$, ϕ rises to a maximum value as θ increases and then sinks back to $\phi=0$ when $\theta=\pi$. As θ completes the circle, ϕ traverses the same path in the negative direction. Accordingly, **P** rises from $\mathbf{P}(\theta=0)=(1,0)$ along the circumference of the circle to an extreme value, returns to $\mathbf{P}(\theta=\pi)=(1,0)$, and then traces the same path in the negative sense, as shown in Fig. 2(b) for $h=0.33$ and $h=0.10$. In contrast to the behavior at higher fields, for $h<\frac{1}{2}$ the entire path is traced only once for each cycle of θ. However, $\mathbf{P}(\theta=0)$ and $\mathbf{P}(\theta=\pi)$ still coincide.

Summarizing, the main features of the magnetoresistance points **P** of a single-domain uniaxial film in a rotating magnetic field are: (1) all points fall on a

[7] D. O. Smith, J. Appl. Phys. **29**, 264 (1958).

single circle although the circle may not be fully traversed for small h; (2) for the full turn of θ at fixed h the **P** trace is covered twice at high fields and only once at low fields, with the points **P** for $\theta=0$ and $\theta=\pi$ coinciding for all values of h.

In a sample of nonuniform magnetization the same type of behavior occurs in each domain and experimental measurements are averages over all the domains. Measurements in a field sufficiently high to overcome the anisotropies must reflect the behavior discussed here. The high-field circle, and the high-field behavior, can therefore be used as reference and for establishing the single-domain values of the parameters of Eqs. (1) and (4).

III. EXPERIMENTAL RESULTS

This section presents measurements of **P** on very thin films of nickel, obtained upon varying θ at fixed h, and upon varying h at fixed θ.

The films, about 100 Å thick, 0.4×2.5 cm, were prepared by evaporation in a manner reported elsewhere,[8,9] at a deposition rate of 10 Å/sec, with the substrate at 80°C, and no aligning field. e_1 was determined across two electrodes on the same side along the film, while the potential difference between their electrically determined midpoint and a centrally opposed third contact gives e_2.

The detailed low-field behavior of the magnetoresistance involves changes less than one hundredth of the radius of the saturation-field circle, requiring for e_1 a resolution $\Delta\rho/\rho$ of approximately 0.03%.[6] By using a carefully constructed 500-cps potentiometer to balance the large constant longitudinal signal, amplification and observation of the smaller variable part is achieved with an overall sensitivity of about 10^{-8} v. To assure that the observed variations are due to $\Delta\rho$ rather than

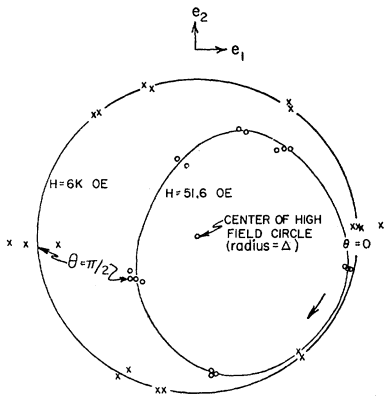

FIG. 3. Magnetoresistance of nickel film, at two large magnetic fields H rotating in the film plane, in terms of the longitudinal and transverse resistivities e_1 and e_2. The arrow indicates the direction of increasing field angle θ to the current direction.

[8] R. Coren and H. J. Juretschke, J. Appl. Phys. **28**, 806 (1957).
[9] E. C. Crittenden, Jr., and R. W. Hoffman, Revs. Modern Phys. **25**, 310 (1953).

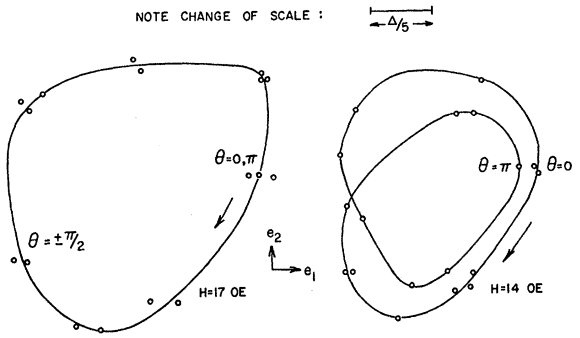

FIG. 4. Magnetoresistance of the film of Fig. 3, at two lower fields. The scale is expanded, and the two traces, actually in the same region of the e_1–e_2 plane, have been separated.

ρ, temperature constancy better than $\frac{1}{10}$°C during a set of measurements is required, and was obtained by immersing the sample in a stoppered Dewar filled with Dow Corning silicone oil (type 200) and enclosed in a region of "dead" air. All measurements were made at room temperature.

Accurate positioning of the film in the applied field assured a negligible out-of-plane component of **M** at even the highest fields of about 6000 gauss. Low magnetic fields were produced by a modified Helmholtz coil, constructed according to the calculations of Garrett,[10] which gave a measured field uniformity of 0.01% over the film region. Before taking data, the field is cycled at least once through 360°.

The experimental variation of **P** as magnetic fields of successively smaller magnitudes are rotated through a full circle is shown in Figs. 3–5, for a representative nickel film. This film has an area resistivity $\rho/t=33$ ohms/sq, an estimated thickness of 80 Å, and a saturation magnetoresistive anisotropy $\Delta\rho/\rho=1.0\%$.

The highest field trace in Fig. 3 is the expected single-domain circle, with $\theta=\phi$; the various points recorded for each θ are obtained upon successive rotations $\theta+n\pi$, and their spread gives a measure of the reproducibility of the circle. The low-field trace on Fig. 3 shows appreciable deviation towards the interior of the circle, with the points no longer equally distributed in equal intervals of θ. The full pattern repeats for each change of θ by π and contact seems to be maintained at $\theta\doteq-20°$, suggesting that this is an overall easy direction of magnetization.

Figures 4 and 5 show **P** traces for rotations of **H** of successively smaller magnitude. The individual figures are presented side by side, although actually they are located in the same region of the e_1–e_2 plane. Due to drift of the measuring circuit the relative position of the high and low field figures is uncertain, so that no common reference point is shown, but they are all within the saturation circle. For clarity, their scales have been adjusted; relative sizes can be determined

[10] M. W. Garrett, J. Appl. Phys. **22**, 185 (1958).

from the bar included in each figure, which denotes a length equal to one-fifth of the radius of the high-field circle.

The lowest field traces in Fig. 5 are characterized by small excursion, and by single-valued variation with θ for $0\leq\theta\leq 2\pi$. The transition between high-field 180° symmetry and low-field 360° symmetry, shown in Fig. 4 and the first trace of Fig. 5, is obtained by the continuous separation of the doubly traced circle into two loops. The unfolding of the loops may be examined in detail by following **P** at given θ for different H (at $H=17$, 14, 10.3, and 8.6 oe. the measurements were mostly taken at 30° intervals of θ).

Deviations from the single-domain behavior are also observed when H is cycled at constant θ. Figure 6 shows the results, on another film, of a complete field reversal of 6 koe at $\theta'=0$, $\pi/2$, $\pi/4$, $3\pi/4$, where θ' is measured from the current direction. Judging from the locations of the low-field points, $\theta'\sim\theta+\pi/2$. Again **P** moves into the interior of the circle and only the high-field regions are reversible and show the expected 2θ dependence. $\theta'=\pi/2$ should be compared to Fig. 1(a); the $\theta'=0$ trace gives a circular loop related to that of Fig. 1(b), though not along the saturation field circle. The traces at $\theta'=\pm\pi/4$, corresponding to hysteresis loops with the field at an angle to the easy direction also deviate strongly from single-domain behavior.

The nature of Figs. 3 through 6, and in particular their relation to the single-domain behavior described in Sec. II, permit the following magnetic characterization of the film:

(1) The shrinking of the pattern within the saturation field circle, indicates that the film breaks up into small domains, so that the measurement gives an average over the domains of a partly demagnetized sample. (2) The continuous rather than abrupt change of the pattern with angle indicates that there is no large change of magnetization by domain-wall motion. (3) Since the experimental low-field values fall neither on the circumference, nor at the center of the saturation circle, the film shows an over-all preferred direction of magnetization. (4) Since the points for $\theta=0$ and $\theta=\pi$ along this magnetically preferred axis do not coincide at all fields, all domains cannot have the same easy axis direction. (A distribution of anisotropies in magnitude but not in direction will not produce this effect because the magnetization of each domain will have either the same or opposite direction in both field situations, regardless of the value of anisotropy. This leads to the same point **P**.)

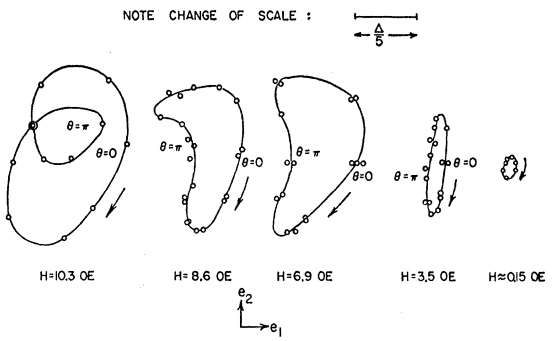

FIG. 5. Magnetoresistance of the film of Figs. 3 and 4 at five lowest fields.

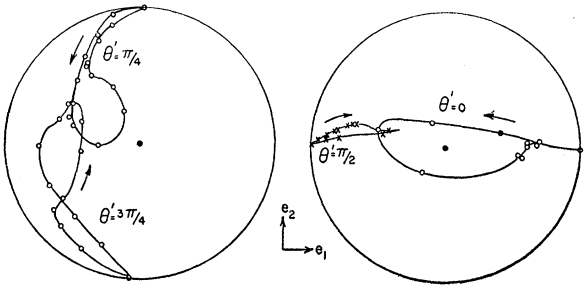

FIG. 6. Magnetoresistance hysteresis of nickel film, with magnetic field cycled between ±6 koe at constant angle θ' with respect to current. The cycle starts at maximum field on the saturation circle, and the magnetoresistance point $\mathbf{P}=(e_1,e_2)$ moves in the direction of the arrows.

IV. MAGNETIC AND ELECTRICAL PROPERTIES OF A MULTIDOMAIN MODEL

Many models of multidomain films having the preceding minimum properties may be constructed. A convenient choice, requiring no special assumptions and amenable to computational treatment, is the model proposed recently by Methfessel and Thomas[11] in connection with the interpretation of other magnetic film properties. It assumes the film to be composed of many small, independent domains, each containing two contributions to the anisotropy energy: a uniaxial energy whose axis orientation is common to all domains, and a local uniaxial anisotropy whose direction differs from one domain to another such as to lead to an isotropic distribution of local anisotropy axes in the film plane. In this section the magnetic and electric properties of that model are formulated and computed, assuming magnetization changes by domain rotation only.

We first consider the behavior of a single domain subject to two uniaxial anisotropy energies. If θ, ϕ, and α denote, respectively, the direction of the external field **H**, the magnetization **M**, and the local anisotropy axis with respect to the common uniaxial easy direction, the magnetic free energy takes the form

$$F=K_1\sin^2\phi+K_2\sin^2(\alpha-\phi)-HM\cos(\theta-\phi). \quad (7)$$

K_1 is the anisotropy energy of the common axis, and K_2 that of the local axis. As pointed out by Wohlfarth and Tonge,[12] Eq. (7) ignores the real crystalline energy. This term will be omitted as the high stress found in thin films produces an anisotropy energy several times

[11] H. Thomas and S. Methfessel (private communication).
[12] E. P. Wohlfarth and D. G. Tonge, Phil. Mag. **2**, 1333 (1957).

greater than the crystalline anisotropy, particularly where no attempt at ordering has been made. Minimizing Eq. (7) with respect to ϕ defines the local equilibrium of **M**. The resulting equation for ϕ,

$$K_1 \sin 2\phi + K_2 \sin 2(\phi-\alpha) = HM \sin(\theta-\phi), \quad (8)$$

may be formally reduced to Eq. (5), describing single axis behavior, by a transformation introducing equivalent uniaxial parameters. Let us introduce the equivalent anisotropy field parameter A and the equivalent easy axis direction β, both defined as functions of α, the local easy axis direction, and of the relative anisotropy constant $K=K_2/K_1$:

$$A^2 = 1+K^2+2K\cos 2\alpha, \quad (9a)$$

$$\tan 2\beta = K\sin 2\alpha/(1-K\cos 2\alpha). \quad (9b)$$

By referring the directions of **H** and **M** to β

$$\gamma=\theta-\beta, \quad \eta=\phi-\beta, \quad (9c)$$

Eq. (8) takes the form

$$\sin 2\eta = (2h/A)\sin(\gamma-\eta), \quad (10)$$

where the reduced field h is, as before,

$$h = HM/2K_1 = H/H_K. \quad (11)$$

Thus, the behavior of a single domain of free energy of the form Eq. (7) is fully equivalent to that of a truly uniaxial domain with its easy axis along β, and anisotropy energy K_1A.

All properties related to the magnetic behavior of our multidomain model can now be computed as averages of the properties of the distribution of equivalent uniaxial domains. For $K=\infty$ one has an isotropic distribution of uniaxial domains, all with common anisotropy energy, i.e., all directions are equivalent. When $K>1$, the uniform distribution of α leads, according to Eq. (9b), to a nonuniform angular distribution of equivalent-domain axis directions β, the anisotropy energy K_1A also varying with β. For $K<1$, the full range of β is covered twice in the full range of α, leading to two nonuniform angular distributions of equivalent-domain axes, with each branch having a different value of A. $K=0$ is the single-domain case.

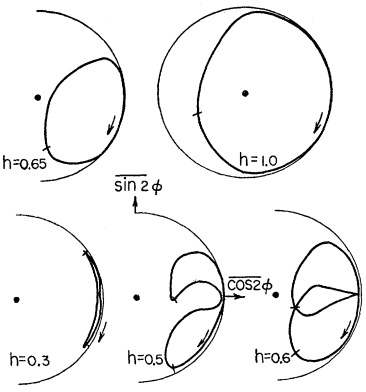

FIG. 7. Theoretical magnetoresistance traces for multidomain model discussed in text, for $K=0.3$ at five relative fields rotating in the film plane. Current and common easy axis are along $\phi=0$, and markers indicate points at which the applied field is at right angles to the current. The high-field circle is also shown.

The qualitative features of the hysteresis loops of the multidomain model follow from the fact that the distribution in angle and anisotropy energies causes the domains to switch at different values of reverse applied field. This produces a rounding of the loop in the common easy direction, and a loss of reversibility along the common hard direction, both effects increasing with K. Detailed calculations have confirmed these features.

The observed electrical behavior of a multidomain film results from the current distribution which must satisfy Eq. (1) subject to continuity requirements within and between the various domains. Since $\Delta\rho/\rho$ is very small, the current flow is always nearly uniform, and to first order in this quantity, the resistance of multidomain samples depends only on the fractional distribution of domains with any given resistance, rather than on their detailed arrangement. Hence, to first order in $\Delta\rho/\rho$, the electrical behavior of a multidomain film is given by the straightforward average of the angles occurring in Eq. (2):

$$\langle\cos 2\phi\rangle_{\rm av} = \frac{1}{\pi}\int_{-\pi/2}^{\pi/2} \cos 2\phi(\alpha)\,d\alpha,$$

$$\langle\sin 2\phi\rangle_{\rm av} = \frac{1}{\pi}\int_{-\pi/2}^{\pi/2} \sin 2\phi(\alpha)\,d\alpha. \quad (12)$$

Only in some limiting cases can these integrals be evaluated analytically. Thus, for a sufficiently large constant external field h rotating in the film plane the entire magnetization will follow the field and we get the single-domain behavior of Fig. 1. At low h the magnetic history of the sample is required for defining correct averages and reproducible measurements. We shall specify that the film has always been brought from saturation along the common easy axis to the desired low field before this is rotated and measurements are taken. For h so low that no switching occurs, approximate analytic expressions can be obtained for Eq. (12) in the extreme ranges of K (for $h\ll 1$):

$$K\ll 1, \quad \langle\cos 2\phi\rangle_{\rm av} = 1-K^2-h^2+h^2\cos 2\theta, \quad \langle\sin 2\phi\rangle_{\rm av} = 2h\sin\theta - h^2\sin 2\theta; \quad (13a)$$

$$K\gg 1, \quad \langle\cos 2\phi\rangle_{\rm av} = 1/2K + (8h/3\pi K)\cos\theta, \quad \langle\sin 2\phi\rangle_{\rm av} = (4h/3\pi K)\sin\theta. \quad (13b)$$

Equations (13a) and (13b) show that at low h the magnetoresistance exhibits essentially a θ dependence rather than a 2θ dependence, for all K. At low K, the P traces are almost independent of K, are elongated along e_2, and are near the circumference of the saturation circle. At high K, the trace is an ellipse, elongated along e_1, with an axial ratio of 2, and is well in the interior of the saturation circle.

Exact curves for intermediate values of h and K have been obtained by numerical computation. Figures 7 and 8 show the magnetoresistance **P** traces for $K=0.3$ and $K=2.0$, respectively, at various values of h. In all cases the points $\theta=0, \pi$ lie on the e_1 axis. At low fields the curves are as described above. At larger h double loops appear, then overlap, and finally coalesce to approach asymptotically the saturation circle. The asymmetry of the loops is determined by the direction of rotation of the applied field.

Figure 9 shows the **P** traces for a multidomain film governed entirely by local anisotropy ($K=\infty$). The deviation from isotropic demagnetization is the result of the specified magnetic history preceding rotation of the applied field. The case of zero local field ($K=0$) is the single-domain case discussed in Sec. II.

Similar calculations have also been made varying h at constant θ. In the description of the single-domain constant-angle magnetoresistance of Fig. 1 it was implied that the field angle differs slightly from 0 or $\pi/2$ in order that **M** have a definite tendency to turn in one direction rather than to split into oppositely rotating parts. Because of the dispersion of axes the rotational behavior of our multidomain model becomes sensitive to the exact value of this misalignment. Since $\sin 2\beta_{\max}=K$, the misalignment at low K need only be a few degrees for complete unidirectional rotation. For larger K the greater angular distribution of equivalent easy axes requires a correspondingly larger misalignment. β ranges over $\pm 90°$ for $K>1$, and then complete unidirectional rotation cannot be achieved. The misalignment governs the fractions rotating in opposite directions.

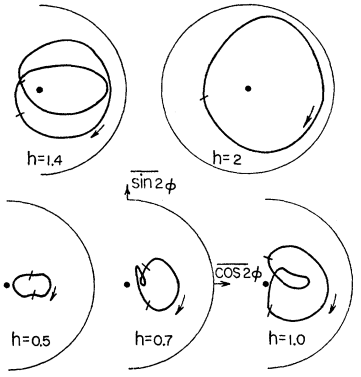

FIG. 8. Theoretical magnetoresistance traces for multidomain model with ratio of local to common anisotropies $K=2.0$. Specification of axes, rotation direction, and angular markers follows that of Fig. 7.

The solid curves in Fig. 10 show the results of numerical calculations for the case $K=2$ assuming that, with the field at $\theta=0$ or $\pi/2$, those domains with $90°>\beta>-13°$ all rotate in one direction and those with $-13°>\beta>-90°$ in the other. This is not exactly equivalent to a misalignment of 13°, but in view of the arbitrariness involved in the misalignment and K value chosen, it is sufficient to illustrate the point. An actual misalignment will affect the high-field points more than the low-field points on this diagram; the dashed curves are sketched in to indicate the probable form of the true curve. These curves bear a great resemblance to those of Fig. 6 except for a clockwise rotation of about 155°. This suggests that the film measured for Fig. 6 has its magnetic axis about 77° from the current direction.

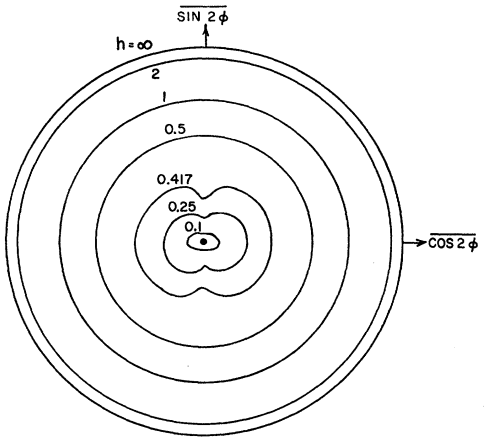

FIG. 9. Theoretical magnetoresistance traces for multidomain model governed by isotropic distribution of local anisotropy axes ($K=\infty$). For each trace, the field h is approached from $h=\infty$ along the easy axis $\phi=0$, and then rotated through 360° in the film plane.

It is apparent that the dominant features of Figs. 7–10 reproduce qualitatively the experimental behavior shown in Figs. 3–6 with respect to both shape and location of the **P** traces. This agreement indicates that our theoretical model contains the necessary basic features to account for the observable properties. The next section examines the degree to which detailed analysis of the experimental data in terms of the model is possible.

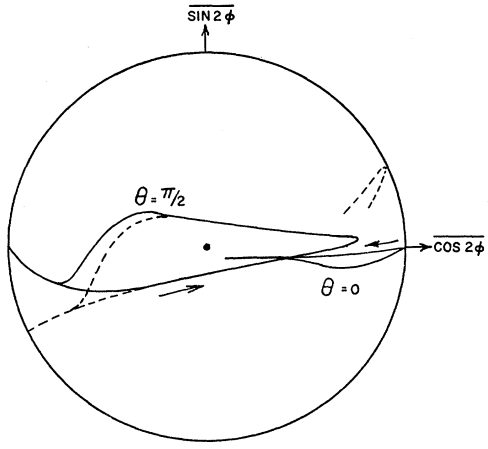

FIG. 10. Theoretical magnetoresistance traces for magnetic field cycled at constant angle θ, for $K=2$. The solid curves are based on the assumption that the division into domains rotating in opposite sense is the same as that resulting from a field misalignment of 13°. The dashed curves suggest the true shape.

V. DISCUSSION

A full interpretation of the experimental data in terms of the proposed model requires that all measurements are explainable in terms of a single parameter K. It is found, however, that different methods of evaluating K from the experimental data do not agree and it is worthwhile to present these methods, and to examine the different results obtained, for the light they throw on the limitations of the model.

One quantitative measure of K may be obtained from the magnetoresistance at zero field. For $h=0$, exact evaluation of Eq. (12) gives

$$\langle\cos 2\phi_0\rangle_{\text{av}}=(1-K)E_1(x)/\pi+(1+K)E_2(x)/\pi, \quad \langle\sin 2\phi_0\rangle_{\text{av}}=0, \quad (14)$$

where $x=K^{\frac{1}{2}}/(1+K)$, and $E_1(x)$, $E_2(x)$ are complete elliptic integrals of the first and second kind, respectively. The data for our films give the value $K=1.4$.

Once K is known, the model predicts the shape and size of the magnetoresistance traces at all relative fields h. In the neighborhood of K found above, however, the theoretical curves (Figs. 7 and 8) are between 30 and 75% larger, relative to the saturation circle, than the experimental ones. Since the figure size at given h becomes smaller for larger K, the observed sizes argue for a much larger value of K. On the other hand, the vertically elongated elliptical shape of the experimental traces at the two lowest fields is intermediate between the low- and high-K shapes of Figs. 7 and 8, and is characteristic of a value $K\lesssim 1$.

Finally, the parameter K may be estimated from the range of fields in which the figure shapes indicate that partial rotational switching occurs. The beginning of rotational switching at low fields is accompanied by significant departures of the figure shape from that of Eq. (13)—it is observable in Fig. 5 between $H=6.9$ oe and $H=8.6$ oe. Rotational switching is complete when the figure is fully symmetric in 2θ—occurring in Fig. 4 between 14 and 17 oe. Theoretically, these two limits correspond to the fields at which regions of lowest and highest equivalent uniaxial anisotropy may switch. Since rotational switching in a single-uniaxial domain first occurs at $H_K/2$, the limiting equivalent-uniaxial anisotropy fields [Eq. (9(a)], combined with the average field values discussed above, lead to the equations

$$|1-K|H_K/2=8 \text{ oe}, \quad |1+K|H_K/2=16 \text{ oe}, \quad (15)$$

which have the two solutions ($K=\frac{1}{3}$, $H_K=24$ oe) and ($K=3$, $H_K=8$ oe). Hence the figure characteristics with respect to switching are compatible with low and high K.

Obviously, a single K value is in conflict with one or another of the features of the observed curves. Since the different characteristics chosen are, in fact, more sensitive to either high- or low-K domains, it is likely that the discrepancy is traceable to the existence of a distribution of K values in the films under study. This possibility, and the range of the distribution, may be explored by considering two values of K, K_a and K_b, with $K_a\gg 1\gg K_b$, present in fractions of f and $(1-f)$. In fields small enough that no switching occurs the description of such a composite model follows from Eq. (13). By relating the height, width, and location of the observed low-field figure to a weighted sum of the first-order terms of Eqs. (13a) and (13b) the three parameters K_a, h, and f may be determined. K_b is then estimated from a second-order solution using the other three parameters and the exact zero-field relations of Eq. (14). Applying this procedure to the experimental curve at 3.5 oe, we obtain the values $f=\frac{2}{3}$, $K_a=5$, $H_K=15$ oe, $K_b=0.2$.

The actual numerical values so obtained are uncertain because of some latitude in curve fitting, but their general range is as anticipated. They are also compatible with the observed figure sizes and agree roughly with the limits of rotational switching if one amends Eq. (15) to take into account that the fields at which the first and last domains switch are smaller and larger, respectively, than the fields at which switching is observed to start or to be complete. The agreement is further improved by allowing a range of anisotropy fields H_K.

We conclude, therefore, that the nickel films discussed here can be adequately described as having regions of large K and regions of small K. The significant range of equivalent uniaxial anisotropy fields is from zero to about 32 oe and the corresponding range of values of K_1 and K_2 is between zero and 16 M_0.

It is possible that, rather than describing a real effect, part of the distribution of K values is an expression of other shortcomings of the model. Thus, coupling between domains, which may arise from internal exchange or may be due to stray fields from the various domains,[13] would change the behavior from that given by the equilibrium of Eq. (8). In addition, it may reflect effects due to magnetic change by domain-wall motion, which has been ignored in these calculations. A calculation including domain-wall motion leads to the conclusion that magnetization rotation should be the dominant mechanism in films with a large range of anisotropy strengths or directions, while for films with a small distribution wall motion is expected to play a greater role. Magnetoresistance measurements on permalloy films with small K value[14] have been shown to be in agreement with the extended theory. While wall motion does not play a major role in the nickel films it may contribute to an apparent K distribution, and will complicate the behavior and analysis at low and intermediate fields.

One other observation may be made concerning the effect of domain walls in thin films on the conduction phenomena under study here. It has been shown by

[13] D. O. Smith and K. J. Harte, Lincoln Laboratory Report 53G-0061, (unpublished).

[14] R. L. Coren and H. J. Juretschke, J. Appl. Phys. **32**, 292S (1961).

Néel[15] and others that in films below a certain thickness the magnetization in a domain wall rotates in the plane of the film rather than across it, as in the case of Bloch domain walls. In nickel the computed critical thickness is in the neighborhood of 300 Å. As a result, when averages are taken over all local anisotropy directions, Néel walls contribute as though they were regions of continuously varying α. This is especially important since these walls become quite broad in very thin films and, as the high degree of surface and interior roughness limits the domain size, may even be comparable to the domains themselves.

The origin of the local and common anisotropies of the model observed in the film is not known, but the following observations suggest that both are partly related to strains existing in the films: (a) The value of K of unannealed films (4 to 5) may be reduced by anneal at 275° to $K\sim1.4$; (b) K approaches zero at liquid nitrogen temperature; (c) K can be reduced by flexing of film and substrate; (d) permalloy, noted for single-domain behavior, has K near zero. Not enough measurements have been taken to determine in each case whether K changes because of K_1 or K_2, but it appears likely that a reduction of K_2 is operative in (a), while K_1 is increasing in (b) and (c); (d) implies a small value of K_2. K_1 is probably associated with strains due to differential thermal expansion. While this is nominally an isotropic effect, strains in a finite size film on a finite thin substrate are determined by film and substrate geometry and may show preferential directions leading to magnetic anisotropy. The results (a) and (d) suggest that K_2 is caused by microstrains.[9] These two strain types are also distinguishable in Hall effect measurements.[16]

[15] L. Néel, Compt. rend. **241**, 533 (1955); S. Methfessel, S. Middelhoek, and H. Thomas, IBM J. Research Develop. **4**, 96 (1960).

[16] R. L. Coren, Suppl. J. Appl. Phys. **33**, 1168 (1962).

VI. CONCLUSIONS

We have shown that systematic magnetoresistance measurements of thin films are useful in identifying the salient characteristics of the films' magnetic domain structure. Though the main features we have observed are common to the group of films under study here, the specific experimental data presented probably do not apply to all nickel films, particularly those very differently prepared. Nevertheless, the results show that there exist in nickel films domain structures of some complexity.

The essential feature of the film model used in interpreting the data is the angular distribution of anisotropy axes. While a distribution of anisotropy strengths is needed to obtain detailed quantitative agreement between theory and experiment, the qualitative behavior is determined entirely by the reduction in symmetry associated with the angular distribution. It should be emphasized that other specific models[17] may also yield the same qualitative behavior. Any multidomain film is founded upon a supposed nonuniformity of some property of the film. Our particular model emphasizes that on a microscopic scale there are no fundamental directional preferences so that the local anisotropy axes are distributed uniformly in direction. The common directional anisotropy is everywhere superimposed on this isotropic pattern. The model has the computational advantage of having only a single adjustable parameter K, but, as shown by our results, this may be too restrictive for actual films. The extent to which the model presents at least a useful first approximation remains to be tested by further comparison between its predictions and experiment.

[17] K. J. Harte, J. Appl. Phys. **31**, 283S (1960); E. P. Wohlfarth, J. Appl. Phys. **30**, 117S (1959).